In vivo Ca^{2+} imaging reveals that decreased dendritic excitability drives startle habituation

Kurt C. Marsden[1] and **Michael Granato**[1]

[1]Department of Cell and Developmental Biology; University of Pennsylvania Perelman School of Medicine; Philadelphia, PA, 19104, USA

Summary

Exposure to repetitive startling stimuli induces habituation, a simple form of learning. Despite its simplicity, the precise cellular mechanisms by which repeated stimulation converts a robust behavioral response to behavioral indifference are unclear. Here, we use head-restrained zebrafish larvae to monitor subcellular Ca^{2+} dynamics in Mauthner neurons, the startle command neurons, during startle habituation *in vivo*. Using the Ca^{2+} reporter GCaMP6s we find that the amplitude of Ca^{2+} signals in the lateral dendrite of the Mauthner neuron determines startle probability and that depression of this dendritic activity rather than downstream inhibition mediates short-term habituation mediates glycine and N-methyl-D-aspartate (NMDA) receptor dependent short-term habituation. Combined, our results suggest a model for habituation learning in which increased inhibitory drive from feedforward inhibitory neurons combined with decreased excitatory input from auditory afferents decreases dendritic and Mauthner neuron excitability.

Introduction

To efficiently navigate their environments, animals filter sensory information such that they attend to salient stimuli while ignoring irrelevant ones. This task requires the nervous system to establish and modify behavioral thresholds to ensure that the behavioral response to a stimulus is appropriate to the environmental context. A prime example of this is habituation, a non-associative form of learning (Thompson and Spencer, 1966) in which repeated inconsequential stimuli elicit a progressive decline in the behavioral response (Groves and Thompson, 1970; Rankin et al., 2009; Thompson and Spencer, 1966). Deficits in habituation are observed in complex brain disorders including schizophrenia (Meincke et al., 2004; Swerdlow et al., 2006) and autism (Dinstein et al., 2012; Kleinhans et al., 2009), yet the neural circuit mechanisms that mediate this behavioral plasticity remain unclear.

Habituation of the acoustic startle response is well documented in mammals and fish, and it displays similar neuropharmacological modulation in both groups (Carey et al., 1998; Halberstadt and Geyer, 2009; Wolman et al., 2011), suggesting that key mechanisms underlying habituation are evolutionarily conserved. In both adult goldfish and in larval zebrafish a single pair of bilateral reticulospinal neurons, the Mauthner cells (M-cells), serve as the so-called 'command neurons' of the startle response (Korn and Faber, 2005), as they are active only during these fast startle responses and without them fast startle behaviors are abolished (Burgess and Granato, 2007; Satou et al., 2009). Moreover, several studies have implicated M-cells and giant neurons in the mammalian reticular formation, the functional equivalent of the M-cell system, in startle habituation (Aljure et al., 1980; Roberts et al., 2011; Simons-Weidenmaier et al., 2006; Weber et al., 2002), indicating that regulation of M-cell activity is likely to be central to startle modulation such as habituation learning.

Results

To study circuit dynamics during acoustic startle habituation we established a method to simultaneously monitor startle circuit activity and behavior in 5-day post-fertilization (dpf) zebrafish larvae. The larval zebrafish startle circuit is simple and accessible, with hair cells in the otic vesicle stimulating eighth (VIII) nerve fibers that directly activate the M-cell at mixed chemical and electrical synapses (Yao et al., 2014). The M-cell then triggers contralateral spinal motor neurons to contract body wall muscle to initiate the stereotyped C-bend response (Figure 1A). To assess M-cell activity we generated a *UAS:GCaMP6s* transgenic line and crossed these fish with the *Gal4FF-62A* line that selectively labels the M-cells (Yamanaka et al., 2013) to optically isolate GCaMP6s-labeled M-cells. Similar to previous studies (O'Malley et al., 1996; Takahashi et al., 2002), transgenic larvae were individually mounted in glass-bottom petri dishes and partially restrained in agarose such that their heads were fixed but their tails were free to move. Tail movements were captured at 500 Hz with a high-speed camera mounted above the stage of a spinning disc confocal microscope. Acoustic-vibrational stimuli were delivered via a small speaker connected to the microscope stage. This non-directional stimulus was calibrated to elicit startle responses to >90% of stimuli while inducing minimal movement of the sample. Larvae were each given 10–11 such stimuli (13 dB) with a minimum of 2 min between stimuli to minimize habituation. Of the 155 total stimuli we observed 7 no-responses (4.5%), while the majority of stimuli resulted in startle responses that could be distinguished by latency. The vast majority of startles (n=137, 88.4% of stimuli) initiated between 4 and 10 ms (short-latency C-bends, SLCs; Figure 1B,C), while the remainder (n=11, 7.1%) initiated between 14 and 46 ms (long-latency C-bends, LLCs; Figure 1C). There was no significant bias in the direction of the behavioral response, with roughly equal numbers of tail flips to the left (n=77) and right (n=60). These data are similar to previous data from free-swimming larvae (Burgess and Granato, 2007), and thus this preparation and the GCaMP6s transgene do not significantly affect larval startle behaviors.

To achieve optimal spatial and temporal resolution, we imaged individual M-cells at 63× magnification and captured a single confocal plane at 20 Hz. During SLCs in which the tail turned contralateral to the imaged M-cell we observed robust Ca^{2+} signals in the M-cell soma, consistent with an M-cell action potential (n=60; mean $\Delta F/F_0$: 2.29 ± 0.11; Figure

1D,E,F). The kinetics of these Ca^{2+} spikes (rise time: 197±4 ms; decay time: 803±20 ms) were similar to those observed using GCaMP6s during a single action potential in mouse visual cortical neurons (Chen et al., 2013). In contrast, we saw very little to no change in GCaMP6s fluorescence during LLCs (n=11; mean $\Delta F/F_0$: 0.15±0.02; Figure 1E,F) regardless of whether the response was contralateral or ipsilateral to the M-cell being imaged. LLC Ca^{2+} signals were indistinguishable from those observed when there was no behavioral response (mean $\Delta F/F_0$: 0.13±0.02, p=0.5133; Figure 1F), supporting previous data showing that M-cells are active only during fast startle responses (Kohashi and Oda, 2008) and are dispensable for LLCs but required for SLCs (Burgess and Granato, 2007; Satou et al., 2009), which hereafter we will refer to as 'startle.' Furthermore, imaging of M-cell Ca^{2+} responses has shown that these signals rely exclusively on Ca^{2+} influx through voltage-gated channels rather than release from internal stores (Takahashi et al., 2002). Thus, GCaMP6s imaging provides an accurate reflection of M-cell membrane potential and its activation state.

During our analysis of M-cell Ca^{2+} responses, we frequently observed changes in fluorescence at the lateral dendrite (Figure 1D, arrowhead), the site of synaptic input from VIII sensory afferents. To determine whether these signals represent subthreshold postsynaptic responses, we presented a series of acoustic stimuli of increasing intensity (−24 to 13 dB) and monitored the M-cell lateral dendrite for changes in Ca^{2+}. We detected activation of the lateral dendrite in the absence of somatic activation even at very low stimulus intensities (Figure 2A–C, Movie S1). Specifically, levels of lateral dendrite activity increased as the intensity of the stimulus increased, while somatic activity was negligible unless the larvae performed a startle (n=270 stimuli in 15 fish; Figure 2C). These data suggest that lateral dendrite Ca^{2+} signals represent graded postsynaptic potentials while somatic Ca^{2+} responses indicate all-or-nothing action potentials. Moreover, a scatterplot of the same lateral dendrite Ca^{2+} responses reveals the level of activity required for startle behavior and that the amplitude of lateral dendrite activation determines the startle probability (Figure 2D), suggesting that plasticity of these dendritic responses may be involved in startle threshold modulation during habituation.

In free-swimming larvae, repeated strong acoustic stimulation rapidly induces habituation (Wolman et al., 2011). We tested head-restrained larvae in this simple learning task with 30 stimuli at 13 dB, the first 5 with a 2 min inter-stimulus interval (ISI) and the final 25 stimuli with a 5 s ISI. We observed robust habituation, as startle frequency decreased from 0.97±0.03 to 0.19±0.04 (n=19 larvae; Figure 3A). One possible mechanism for this behavioral plasticity is that inhibition downstream of the M-cell prevents motor neuron activation. Earlier work has shown that acoustic stimulation can activate both M-cells but that a set of spinal inhibitory neurons downstream of the M-cell, CoLos, prevent the trailing spike from activating motor neurons, ensuring a unilateral behavioral response (Satou et al., 2009). To confirm that inhibition downstream of the M-cell is operational in our system, we imaged both M-cells at 40× in 5 larvae and observed that 29/50 (58%) stimuli at 13 dB elicited bilateral M-cell activation, with the remaining 42% triggering unilateral M-cell responses (Figure 3B). Similarly, when we imaged one M-cell at 63× and analyzed only startle events towards the ipsilateral side of the recorded M-cell, the majority of such events

(56/85; 66%) were associated with robust M-cell responses (mean $\Delta F/F_0$: 2.58±0.12) indistinguishable from those during contralateral startles (Figure 1F). In the remaining 29/85 (33%) ipsilateral startles M-cell activation was negligible (mean $\Delta F/F_0$: 0.14±0.01). These data demonstrate a strong and reliable source of inhibition downstream of the M-cell soma, consistent with the idea that this mechanism is engaged during habituation.

This model predicts that during habituation the M-cell soma continues to be activated but that this is insufficient to trigger startle behavior. To test this prediction we analyzed M-cell Ca^{2+} responses during our 30-stimulus habituation protocol. Contrary to the model, however, the frequency of somatic Ca^{2+} responses, likely representing all-or-nothing action potentials (Figure 2C), followed the behavioral output and decreased rapidly (0.96±0.02 to 0.14±0.06; n=19 fish; Figure 3C,D). To directly test whether CoLo inhibitory interneurons are dispensable for startle habituation, we bilaterally laser-ablated all CoLos caudal to the fifth segment at 2–2.5 dpf using the Tol056 transgenic line that labels CoLos and M-cells with GFP (Satou et al., 2009). Ablations were confirmed by imaging 24 hrs post-ablation (Figure 3E). At 5 dpf, CoLo-ablated larvae showed no difference in startle habituation compared to non-ablated controls when tested in a free-swimming version of the same 30-stimulus assay (control: n=17; CoLo-ablated n=4; Figure 3F). Importantly, startle responses in CoLo-ablated larvae were abnormal in that the tail straightened and shortened (Figure S1A), indicative of bilateral muscle contraction due to the elimination of inhibition that prevents bilateral M-cell activation (Satou et al., 2009). These data provide compelling evidence against a habituation mechanism requiring inhibition downstream of the M-cell soma.

A second possible mechanism is that depression of M-cell lateral dendrite responses prevents M-cell activation during habituation. To measure whether changes in lateral dendrite activity are associated with habituation, we compared activity in habituated and non-habituated larvae. We and others have previously identified the N-methyl-D-aspartate (NMDA) receptor inhibitor MK-801 as a potent inhibitor of short-term habituation in 5 dpf zebrafish (Roberts et al., 2011; Wolman et al., 2011), and we also tested the role of glycinergic inhibition during habituation using the glycine receptor blocker strychnine. 15 min application of MK-801 (500 μM) or strychnine (100 μM) prior to testing dramatically reduced habituation (MK801: 1.0±0.0 to 0.78±0.08, n=8; strychnine: 1.0±0.0 to 0.91±0.09, n=9) compared to DMSO-treated larvae (1.0±0.0 to 0.20±0.05; n=8; Figure 4A). After 5 min rest we gave one more stimulus, and startle responsiveness spontaneously recovered (Figure 4A). These data demonstrate that while CoLo-mediated inhibition downstream of the M-cell is dispensable, other populations of glycinergic neurons are essential for startle habituation. MK-801 treatment did not alter M-cell GCaMP6s properties, as peak fluorescence (Figure 4B) and kinetics (Figure 4C) of Ca^{2+} signals were unchanged. Thus, NMDA receptors contribute minimal Ca^{2+} to GCaMP6s signals in the M-cell. Strychnine caused bilateral muscle contraction (Figure S1B) and also increased the amplitude and decay time of lateral dendrite and somatic Ca^{2+} signals (Figure 4B,C), indicating that glycinergic inhibition shapes M-cell activity.

Next we measured M-cell activity during habituation. In untreated larvae we consistently observed decreases in peak GCaMP6s fluorescence associated with startle responses and M-

cell somatic activation during the habituation protocol (Figure 3D, stim 5 vs. stim 18). Ca^{2+} responses during action potential-like events in which there was a startle response _and_ a strong Ca^{2+} signal in the M-cell soma (>10 SDs above signals when there was no startle response) were significantly decreased (soma: 58.9±2.84%; lateral dendrite: 79.3±1.44%; n=26 larvae; Figure S2A,B). This effect is largely independent of the effects of illumination, as peak F/F_0 decreased only slightly when the imaging laser was on for the same duration as the habituation assay but no acoustic stimuli were delivered (soma: 0.13±6.45%, lateral dendrite: 14.8±6.41%; n=9; Figure S2C,D). Because M-cell soma and lateral dendrite responses did not change when all 30 stimuli were separated by 2 min (Figure S2E,F), the decrease in action potential signals during habituaion is likely due to repeated excitation of GCaMP6s. Because of the high affinity of GCaMP6s for Ca^{2+}, repeated stimulation would reduce GCaMP6s sensitivity, a phenomenon observed with other Ca^{2+} indicators (Takahashi et al., 2002). Critically, Ca^{2+} signals remained robustly detectable above noise.

Lateral dendrite Ca^{2+} responses during habituation were normalized to the curve in Figure S2B, and in strongly habituated, DMSO-treated larvae these signals were decreased by approximately 35%, while in non-habituated, MK-801-treated larvae no significant depression was observed (DMSO: n = 8; MK-801: n = 8; $p < 0.0001$, 2-way ANOVA; Figure 4D). Lateral dendrite signals recovered to baseline after 5 min rest. Finally, lateral dendrite signals in non-habituated strychnine-treated larvae were decreased from their baseline but remained elevated relative to DMSO controls (strychnine: n = 6; $p < 0.0001$, 2-way ANOVA; Figure 4D). These data indicate that habituation results from an NMDA and glycine receptor dependent decrease in dendritic excitability below a critical threshold.

Repetitive stimuli at different ISIs can engage different mechanisms to produce habituation (Broster and Rankin, 1994; Wicks and Rankin, 1996), so to test whether depression of lateral dendrite activity is a general mechanism for larval zebrafish startle habituation we doubled the ISI to 10 s. As before, DMSO-treated larvae strongly habituated but more slowly (Wolman et al., 2011), while MK-801-treated larvae showed very little habituation (Figure S3A). Similar to the 5 s ISI assay, lateral dendrite signals decreased approximately 35% in DMSO controls, while MK-801-treated larvae showed no change in dendritic activity (DMSO: n = 6; MK-801: n = 8; $p < 0.0001$; Figure S3B). Startle behavior and dendritic activity recovered for both groups following the rest period. These data illustrate the plasticity of the startle circuit and reveal a general mechanism for startle habituation: depression of M-cell lateral dendrite excitability.

Discussion

Behavioral plasticity such as learning is characterized by changes in neuronal activity (Bliss and Lomo, 1973; Castellucci and Kandel, 1974). While these changes are often thought to be input-specific and limited to a subset of synapses on a given neuron (Harvey and Svoboda, 2007; Hebb, 1964; Wen and Barth, 2011), how such subcellular modulation of activity regulates behavioral output is difficult to assess in behaving animals. In this study we utilize a non-invasive optical approach to record changes in subcellular neuronal activity in a behaving vertebrate during a simple learning task. Using this approach we identify the

M-cell lateral dendrite as the site of startle threshold regulation and demonstrate that depression of dendritic excitability drives habituation learning.

Advances in Ca^{2+} indicators and microscopy have increased our understanding of the neuronal mechanisms of some forms of learning (Ahrens et al., 2012; Cichon and Gan, 2015), although *in vivo* evidence for the mechanisms underlying vertebrate startle habituation is incomplete. Habituation of the *Aplysia* tactile gill and siphon withdrawal reflex appears to be driven by homosynaptic depression at the sensorimotor synapse (Glanzman, 2009). Similarly, work in hatchet fish suggests that acoustic startle habituation could result from decreased synaptic transmission at the VIII-M-cell synapse (Aljure et al., 1980). Supporting this mechanism, *in vitro* data from rat brain slices suggests that presynaptic depression at axon terminals of sensory afferents onto giant caudal pontine reticular nucleus (PnC) neurons, the mammalian analogs of the M-cells, might underlie short-term startle habituation (Simons-Weidenmaier et al., 2006; Weber et al., 2002). Recent data from larval zebrafish shows that increasing electrical stimulation of auditory hair cells triggers stepwise increases in M-cell excitatory postsynaptic potentials (EPSPs), indicating recruitment of additional sensory afferents and activation of more club endings on the M-cell (Yao et al., 2014). Our subthreshold Ca^{2+} imaging data (Figure 2) reflect this pattern, so this is likely part of the mechanism for the graded dendritic responses we observe with increased acoustic stimulation. Depression of these same inputs thus might be involved in the dendritic depression we observe during habituation (Figure 4D). Because dendritic signals still undergo depression in the presence of strychnine, which prevents habituation (Figure 4A and 4D), depression of dendritic excitability is independent of inhibition but is not sufficient to induce habituation. We cannot exclude, however, that when all glycine receptors are blocked changes at sites other than the lateral dendrite may also contribute to startle habituation.

An alternative mechanism for habituation has been proposed based on data from multiple systems. Potentiation of inhibitory synapses is implicated in habituation of the *Aplysia* siphon withdrawal reflex (Bristol and Carew, 2005; Fischer et al., 1997), the crayfish escape response (Krasne and Teshiba, 1995; Shirinyan et al., 2006), and the *Drosophila* proboscis extension response to sweet stimulation (Paranjpe et al., 2012). Similarly, decreased startle responsiveness during a conditioning program similar to habituation is mediated by inhibitory long-term potentiation (iLTP) in the adult goldfish M-cell (Oda et al., 1998).

Three sources of inhibition in the larval zebrafish startle circuit have been identified: 1) CoLos, spinal interneurons activated by M-cell axons that inhibit motor neurons (Satou et al., 2009), 2) glycinergic feedback (FB) inhibitory neurons, which are activated by M-cell firing via Cranial Relay Neurons (CRNs) and inhibit the M-cell at its axon cap (Koyama et al., 2011; Takahashi et al., 2002), and 3) glycinergic feedforward (FF) inhibitory neurons, often called passive hyperpolarizing potential (PHP) neurons (Koyama et al., 2011). Our analysis directly rules out CoLos from the habituation mechanism (Figure 3F), and our data implicating both NMDA receptors and glycine receptors (Figure 4A,D) are inconsistent with a CRN-FB pathway, as this is a cholinergic connection (Koyama et al., 2011). Inhibitory drive from these neurons is also inconsistent with the absence of M-cell somatic activity and depression of lateral dendrite activity we observe during startle habituation (Figure 3,4).

Excitatory spiral fiber (SF) neurons, recently implicated in regulating M-cell firing and startle probablility (Lacoste et al., 2015) can likely be excluded on similar grounds as their input lies downstream of the M-cell soma. FF neurons, on the other hand, receive glutamatergic input from VIII afferents and are known to regulate the startle threshold in adult goldfish (Weiss et al., 2008) and African cichlid fish (Neumeister et al., 2010), and in larval zebrafish these neurons are adjacent to the M-cell lateral dendrite (Koyama et al., 2011) where their input likely influences dendritic responses. Our data are consistent with work in adult goldfish showing that inhibitory synapses on the M-cell are potentiated by repeated stimulation through a partially NMDA receptor-dependent pathway (Korn et al., 1992; Oda et al., 1998). Although we cannot rule out that changes in voltage-gated channels also contribute to dendritic depression during habituation, our data suggest a model in which repeated stimulation of VIII afferents with startling stimuli activates NMDA receptors on the M-cell, resulting in decreased excitatory transmission at these synapses. Simultaneously, activation of NMDA receptors on FF neurons, the M-cell or both produces a strengthening of FF-to-M-cell synapses, resulting in decreased dendritic excitability and reduced startle probability (Figure 4F). These changes in synaptic efficacy may take place through either pre- or post-synaptic mechanisms.

It is important to note that the acoustic startle response in zebrafish is all-or-none (Burgess and Granato, 2007; Kimmel et al., 1974), thus the habituation we describe here is a change in startle probability, not magnitude. Habituation of response probability and magnitude in *C. elegans* following tap stimulation have been demonstrated to rely on different mechanisms (Kindt et al., 2007), and so it will be interesting to test whether this holds true for habituation of other larval zebrafish behaviors that exhibit graded responses such as the O-bend response to changes in illumination (Wolman et al., 2014). The optical method we describe here provides a powerful, non-invasive technique for investigating changes in circuit activity in an intact, genetically tractable vertebrate organism during learning. Future investigations will be able to benefit from this approach using the large library of zebrafish Gal4 lines (Kawakami et al., 2010; Scott et al., 2007) and recently identified mutants with habituation defects (Wolman et al., 2015) to better understand the cellular and molecular program underlying this behavioral plasticity.

Experimental Procedures

Generation and maintenance of zebrafish

UAS:GCaMP6s fish were generated in the Tüpfel longfin (TLF) strain with I-SceI-mediated transgenesis as described previously (Thermes et al., 2002). *Gal4FF-62A* fish were kindly provided by Koichi Kawakami (Yamanaka et al., 2013). Embryos were raised at 29°C on a 14-h:10-h light:dark cycle in E3 media as described previously (Burgess and Granato, 2007). All animal protocols were approved by the University of Pennsylvania Institutional Animal Care and Use Committee. See Supplemental Experimental Procedures for further details.

Combined Ca²⁺ and behavioral imaging

5-dpf zebrafish larvae were embedded in 2% agarose in glass-bottom petri dishes with tails freed by removing agarose distal to the anus. Drugs were prepared at 100× in DMSO. All images were captured with a Leica CTR7000 HS spinning disc confocal microscope using MetaMorph software (Molecular Devices). Acoustic stimuli were delivered with a Behringer A500 amplifier and Visaton SC 5.9 speaker placed on the microscope stage. High-speed images of tail movement were captured with a Dalsa Genie HM640 camera using Streampix5 software (Norpix). Latencies and turn angles were manually analyzed. Free-swimming behavioral analysis of CoLo-ablated larvae was done as described previously (Wolman et al., 2011; 2015). See Supplemental Experimental Procedures for further details.

CoLo interneuron ablations

Targeted cell ablations were done with a MicroPoint laser (Andor) as described previously (Jain et al., 2014). See Supplemental Experimental Procedures for further details.

Data analysis

Images were analyzed with Image J (NIH). Statistical analysis was done using Prism 5 (GraphPad), with all data presented as mean ± SEM and *p* values calculated by 2-tailed *t* tests or one- or two-way ANOVA with post-tests as indicated. See Supplemental Experimental Procedures for further details.

Supplementary Material

Refer to Web version on PubMed Central for supplementary material.

Acknowledgements

References

Ahrens MB, Li JM, Orger MB, Robson DN, Schier AF, Engert F, Portugues R. Brain-wide neuronal dynamics during motor adaptation in zebrafish. Nature. 2012:1–9.

Aljure E, Day JW, Bennett MV. Postsynaptic depression of Mauthner cell-mediated startle reflex, a possible contributor to habituation. Brain Research. 1980; 188:261–268. [PubMed: 7370756]

Bliss TV, Lomo T. Long-lasting potentiation of synaptic transmission in the dentate area of the anaesthetized rabbit following stimulation of the perforant path. J. Physiol. (Lond.). 1973; 232:331–356. [PubMed: 4727084]

Bristol AS, Carew TJ. Differential role of inhibition in habituation of two independent afferent pathways to a common motor output. Learn. Mem. 2005; 12:52–60. [PubMed: 15647595]

Broster BS, Rankin CH. Effects of changing interstimulus interval during habituation in Caenorhabditis elegans. Behav. Neurosci. 1994; 108:1019–1029. [PubMed: 7893394]

Burgess HA, Granato M. Sensorimotor gating in larval zebrafish. J. Neurosci. 2007; 27:4984–4994. [PubMed: 17475807]

Carey RJ, Dai H, Gui J. Effects of dizocilpine (MK-801) on motor activity and memory. Psychopharmacology. 1998; 137:241–246. [PubMed: 9683001]

Castellucci VF, Kandel ER. A quantal analysis of the synaptic depression underlying habituation of the gill-withdrawal reflex in Aplysia. Proc. Natl. Acad. Sci. U.S.a. 1974; 71:5004–5008. [PubMed: 4373738]

Chen T-W, Wardill TJ, Sun Y, Pulver SR, Renninger SL, Baohan A, Schreiter ER, Kerr RA, Orger MB, Jayaraman V, et al. Ultrasensitive fluorescent proteins for imaging neuronal activity. Nature. 2013; 499:295–300. [PubMed: 23868258]

Cichon J, Gan W-B. Branch-specific dendritic Ca(2+) spikes cause persistent synaptic plasticity. Nature. 2015; 520:180–185. [PubMed: 25822789]

Dinstein I, Heeger DJ, Lorenzi L, Minshew NJ, Malach R, Behrmann M. Unreliable evoked responses in autism. Neuron. 2012; 75:981–991. [PubMed: 22998867]

Fischer TM, Blazis DE, Priver NA, Carew TJ. Metaplasticity at identified inhibitory synapses in Aplysia. Nature. 1997; 389:860–865. [PubMed: 9349819]

Glanzman DL. Habituation in Aplysia: the Cheshire cat of neurobiology. Neurobiology of Learning and Memory. 2009; 92:147–154. [PubMed: 19332142]

Groves PM, Thompson RF. Habituation: a dual-process theory. Psychol Rev. 1970; 77:419–450. [PubMed: 4319167]

Halberstadt AL, Geyer MA. Habituation and sensitization of acoustic startle: opposite influences of dopamine D1 and D2-family receptors. Neurobiology of Learning and Memory. 2009; 92:243–248. [PubMed: 18644244]

Harvey CD, Svoboda K. Locally dynamic synaptic learning rules in pyramidal neuron dendrites. Nature. 2007; 450:1195–1200. [PubMed: 18097401]

Hebb DO. The Organization of Behaviour, a Neuropsychological Theory. 1964 D.O. Hebb, ….

Jain RA, Bell H, Lim A, Chien C-B, Granato M. Mirror movement-like defects in startle behavior of zebrafish dcc mutants are caused by aberrant midline guidance of identified descending hindbrain neurons. J. Neurosci. 2014; 34:2898–2909. [PubMed: 24553931]

Kawakami K, Abe G, Asada T, Asakawa K, Fukuda R, Ito A, Lal P, Mouri N, Muto A, Suster ML, et al. zTrap: zebrafish gene trap and enhancer trap database. BMC Developmental Biology. 2010; 10:105. [PubMed: 20950494]

Kimmel CB, Patterson J, Kimmel RO. The development and behavioral characteristics of the startle response in the zebra fish. Dev Psychobiol. 1974; 7:47–60. [PubMed: 4812270]

Kindt KS, Quast KB, Giles AC, De S, Hendrey D, Nicastro I, Rankin CH, Schafer WR. Dopamine mediates context-dependent modulation of sensory plasticity in C. elegans. Neuron. 2007; 55:662–676. [PubMed: 17698017]

Kleinhans NM, Johnson LC, Richards T, Mahurin R, Greenson J, Dawson G, Aylward E. Reduced neural habituation in the amygdala and social impairments in autism spectrum disorders. Am J Psychiatry. 2009; 166:467–475. [PubMed: 19223437]

Kohashi T, Oda Y. Initiation of Mauthner- or non-Mauthner-mediated fast escape evoked by different modes of sensory input. J. Neurosci. 2008; 28:10641–10653. [PubMed: 18923040]

Korn H, Oda Y, Faber DS. Long-term potentiation of inhibitory circuits and synapses in the central nervous system. Proc. Natl. Acad. Sci.U.S.a. 1992; 89:440–443. [PubMed: 1729715]

Korn H, Faber DS. The Mauthner cell half a century later: a neurobiological model for decision-making? Neuron. 2005; 47:13–28. [PubMed: 15996545]

Koyama M, Kinkhabwala A, Satou C, Higashijima S-I, Fetcho J. Mapping a sensory-motor network onto a structural and functional ground plan in the hindbrain. Proc. Natl. Acad. Sci. U.S.a. 2011; 108:1170–1175. [PubMed: 21199937]

Krasne FB, Teshiba TM. Habituation of an invertebrate escape reflex due to modulation by higher centers rather than local events. Proc. Natl. Acad. Sci. U.S.a. 1995; 92:3362–3366. [PubMed: 7724567]

Lacoste AMB, Schoppik D, Robson DN, Haesemeyer M, Portugues R, Li JM, Randlett O, Wee CL, Engert F, Schier AF. A Convergent and Essential Interneuron Pathway for Mauthner-Cell-Mediated Escapes. Curr. Biol. 2015

Meincke U, Light GA, Geyer MA, Braff DL, Gouzoulis-Mayfrank E. Sensitization and habituation of the acoustic startle reflex in patients with schizophrenia. Psychiatry Res. 2004; 126:51–61. [PubMed: 15081627]

Neumeister H, Whitaker KW, Hofmann HA, Preuss T. Social and Ecological Regulation of a Decision-Making Circuit. Journal of Neurophysiology. 2010; 104:3180–3188. [PubMed: 20926612]

O'Malley DM, Kao YH, Fetcho JR. Imaging the functional organization of zebrafish hindbrain segments during escape behaviors. Neuron. 1996; 17:1145–1155. [PubMed: 8982162]

Oda Y, Kawasaki K, Morita M, Korn H, Matsui H. Inhibitory long-term potentiation underlies auditory conditioning of goldfish escape behaviour. Nature. 1998; 394:182–185. [PubMed: 9671301]

Paranjpe P, Rodrigues V, Vijayraghavan K, Ramaswami M. Gustatory habituation in Drosophila relies on rutabaga (adenylate cyclase)-dependent plasticity of GABAergic inhibitory neurons. Learn. Mem. 2012; 19:627–635. [PubMed: 23169996]

Rankin CH, Abrams T, Barry RJ, Bhatnagar S, Clayton DF, Colombo J, Coppola G, Geyer MA, Glanzman DL, Marsland S, et al. Habituation revisited: an updated and revised description of the behavioral characteristics of habituation. Neurobiology of Learning and Memory. 2009; 92:135–138. [PubMed: 18854219]

Roberts AC, Reichl J, Song MY, Dearinger AD, Moridzadeh N, Lu ED, Pearce K, Esdin J, Glanzman DL. Habituation of the C-start response in larval zebrafish exhibits several distinct phases and sensitivity to NMDA receptor blockade. PLoS ONE. 2011; 6:e29132. [PubMed: 22216183]

Satou C, Kimura Y, Kohashi T, Horikawa K, Takeda H, Oda Y, Higashijima SI. Functional Role of a Specialized Class of Spinal Commissural Inhibitory Neurons during Fast Escapes in Zebrafish. J. Neurosci. 2009; 29:6780–6793. [PubMed: 19474306]

Scott EK, Mason L, Arrenberg AB, Ziv L, Gosse NJ, Xiao T, Chi NC, Asakawa K, Kawakami K, Baier H. Targeting neural circuitry in zebrafish using GAL4 enhancer trapping. Nat Meth. 2007; 4:323–326.

Shirinyan D, Teshiba T, Taylor K, O'Neill P, Lee SC, Krasne FB. Rostral ganglia are required for induction but not expression of crayfish escape reflex habituation: role of higher centers in reprogramming low-level circuits. Journal of Neurophysiology. 2006; 95:2721–2724. [PubMed: 16381808]

Simons-Weidenmaier NS, Weber M, Plappert CF, Pilz PKD, Schmid S. Synaptic depression and short-term habituation are located in the sensory part of the mammalian startle pathway. BMC Neurosci. 2006; 7:38. [PubMed: 16684348]

Swerdlow NR, Light GA, Cadenhead KS, Sprock J, Hsieh MH, Braff DL. Startle gating deficits in a large cohort of patients with schizophrenia: relationship to medications, symptoms, neurocognition, and level of function. Arch. Gen. Psychiatry. 2006; 63:1325–1335. [PubMed: 17146007]

Takahashi M, Narushima M, Oda Y. In vivo imaging of functional inhibitory networks on the mauthner cell of larval zebrafish. J. Neurosci. 2002; 22:3929–3938. [PubMed: 12019312]

Thermes V, Grabher C, Ristoratore F, Bourrat F, Choulika A, Wittbrodt J, Joly J-S. I-SceI meganuclease mediates highly efficient transgenesis in fish. Mech. Dev. 2002; 118:91–98. [PubMed: 12351173]

Thompson RF, Spencer WA. Habituation: a model phenomenon for the study of neuronal substrates of behavior. Psychol Rev. 1966; 73:16–43. [PubMed: 5324565]

Weber M, Schnitzler H-U, Schmid S. Synaptic plasticity in the acoustic startle pathway: the neuronal basis for short-term habituation? Eur. J. Neurosci. 2002; 16:1325–1332. [PubMed: 12405993]

Weiss SA, Preuss T, Faber DS. A role of electrical inhibition in sensorimotor integration. Proc. Natl. Acad. Sci. U.S.a. 2008; 105:18047–18052. [PubMed: 19004764]

Wen JA, Barth AL. Input-specific critical periods for experience-dependent plasticity in layer 2/3 pyramidal neurons. J. Neurosci. 2011; 31:4456–4465. [PubMed: 21430146]

Wicks SR, Rankin CH. Recovery from habituation in Caenorhabditis elegans is dependent on interstimulus interval and not habituation kinetics. Behav. Neurosci. 1996; 110:840–844. [PubMed: 8864275]

Wolman MA, Jain RA, Liss L, Granato M. Chemical modulation of memory formation in larval zebrafish. Proc. Natl. Acad. Sci. U.S.a. 2011; 108:15468–15473. [PubMed: 21876167]

Wolman MA, de Groh ED, McBride SM, Jongens TA, Granato M, Epstein JA. Modulation of cAMP and ras signaling pathways improves distinct behavioral deficits in a zebrafish model of neurofibromatosis type 1. Cell Rep. 2014; 8:1265–1270. [PubMed: 25176649]

Wolman MA, Jain RA, Marsden KC, Bell H, Skinner J, Hayer KE, Hogenesch JB, Granato M. A Genome-wide Screen Identifies PAPP-AA-Mediated IGFR Signaling as a Novel Regulator of Habituation Learning. Neuron. 2015; 85:1200–1211. [PubMed: 25754827]

Yamanaka I, Miki M, Asakawa K, Kawakami K, Oda Y, Hirata H. Glycinergic transmission and postsynaptic activation of CaMKII are required for glycine receptor clustering in vivo. Genes Cells. 2013; 18:211–224. [PubMed: 23347046]

Yao C, Vanderpool KG, Delfiner M, Eddy V, Lucaci AG, Soto-Riveros C, Yasumura T, Rash JE, Pereda AE. Electrical synaptic transmission in developing zebrafish: properties and molecular composition of gap junctions at a central auditory synapse. Journal of Neurophysiology. 2014; 112:2102–2113. [PubMed: 25080573]
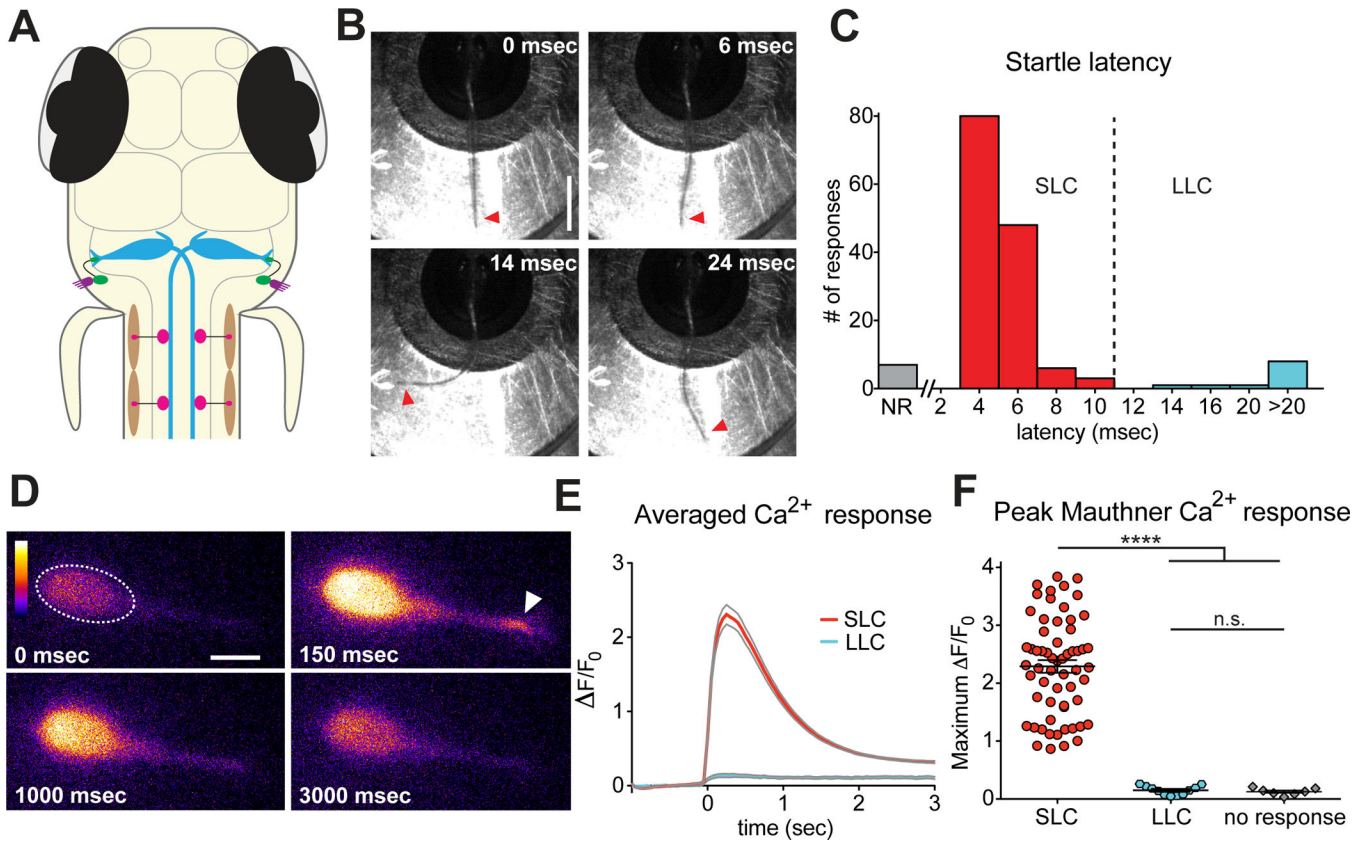
Figure 1. The Mauthner cell is active only during short-latency C-bends and not during long-latency C-bends

(A) The larval zebrafish acoustic startle circuit: hair cells in the otic vesicle (purple), VIII nerve afferents (green), hindbrain Mauthner cells (M-cells, blue), spinal motor neurons (pink) and contraction of muscle (brown). (B) High-speed images (500 Hz) of a short-latency C-bend (SLC) in a head-restrained 5 dpf larva. Arrowheads highlight tail (scale bar 1 mm). (C) Distribution of startle latencies in head-restrained larvae (NR: no response; LLC: long-latency C-bend). (D) Representative example of M-cell activation following acoustic stimulation in a *Gal4FF62a;UAS:GCaMP6s* transgenic larva. Arrowhead highlights lateral dendrite activation. Color scale denotes fluorescence intensity (black: lowest, white: highest; scale bar 10 μm). (E) Averaged traces show change in fluorescence (F) relative to baseline (F_0) for SLC (red) and LLC (blue) responses performed to the contralateral side of the imaged M-cell. Grey lines indicate SEM. (F) Scatterplot of peak F/F_0 values for contralateral SLCs, LLCs and NRs. (****$p<0.0001$, *t* test).
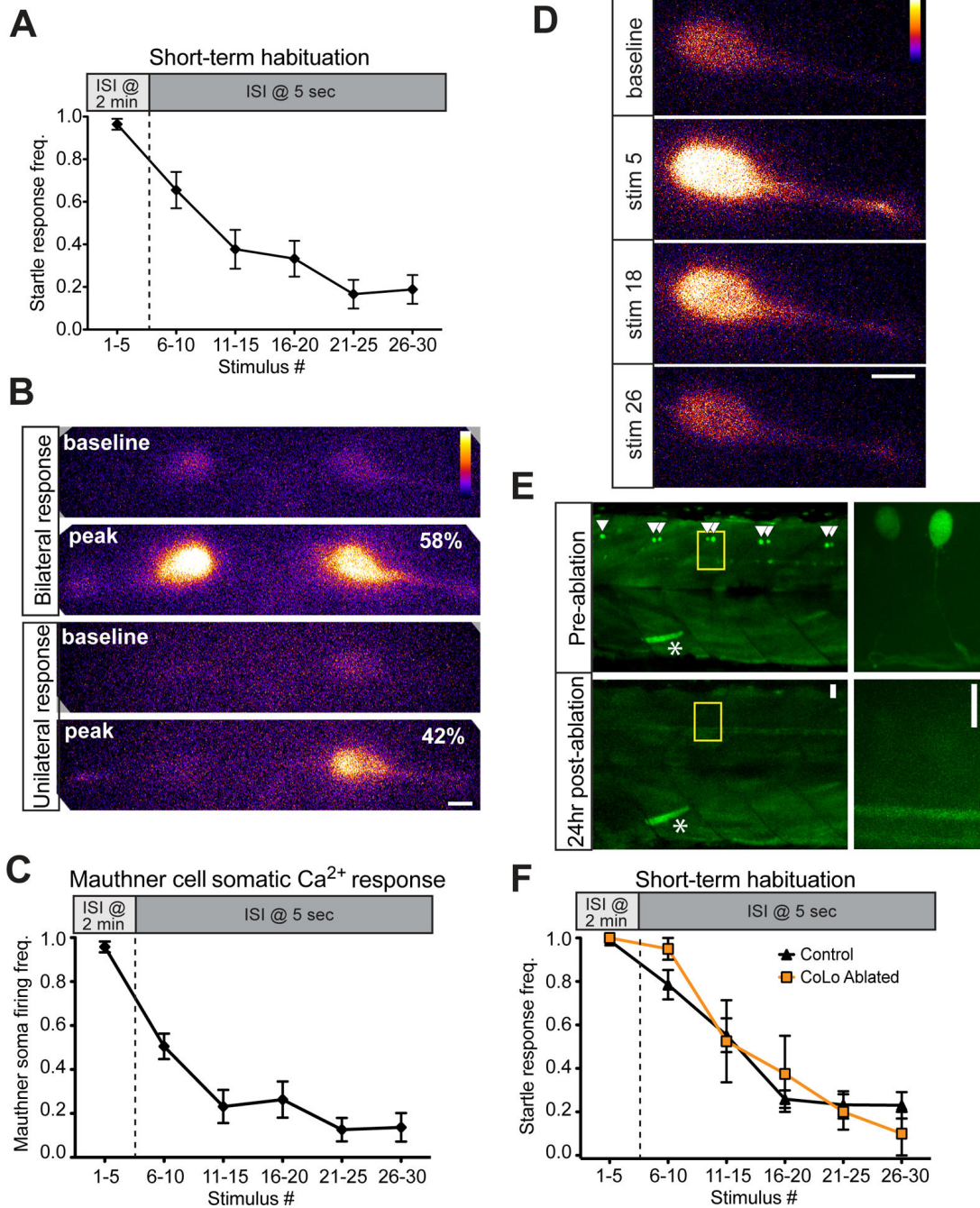
Figure 2. Graded M-cell lateral dendrite Ca^{2+} signals reflect startle probability

(A) Increasing stimulus intensity increases activity at the M-cell lateral dendrite (white dashed line), with no change in somatic (blue dashed line) activity unless a startle is performed (scale bar 10 μm). (B) Representative F/F_0 traces from a single M-cell show graded lateral dendrite responses. Stimuli were calibrated with an accelerometer, with voltage outputs converted to dB using the formula dB=20 log (V/0.775). (C) Grouped F/F_0 data reveal all-or-none somatic activity (blue bars) in startles vs. non-startles regardless of stimulus intensity and graded lateral dendrite activity (white bars; *$p<0.05$, ***$p<0.001$,
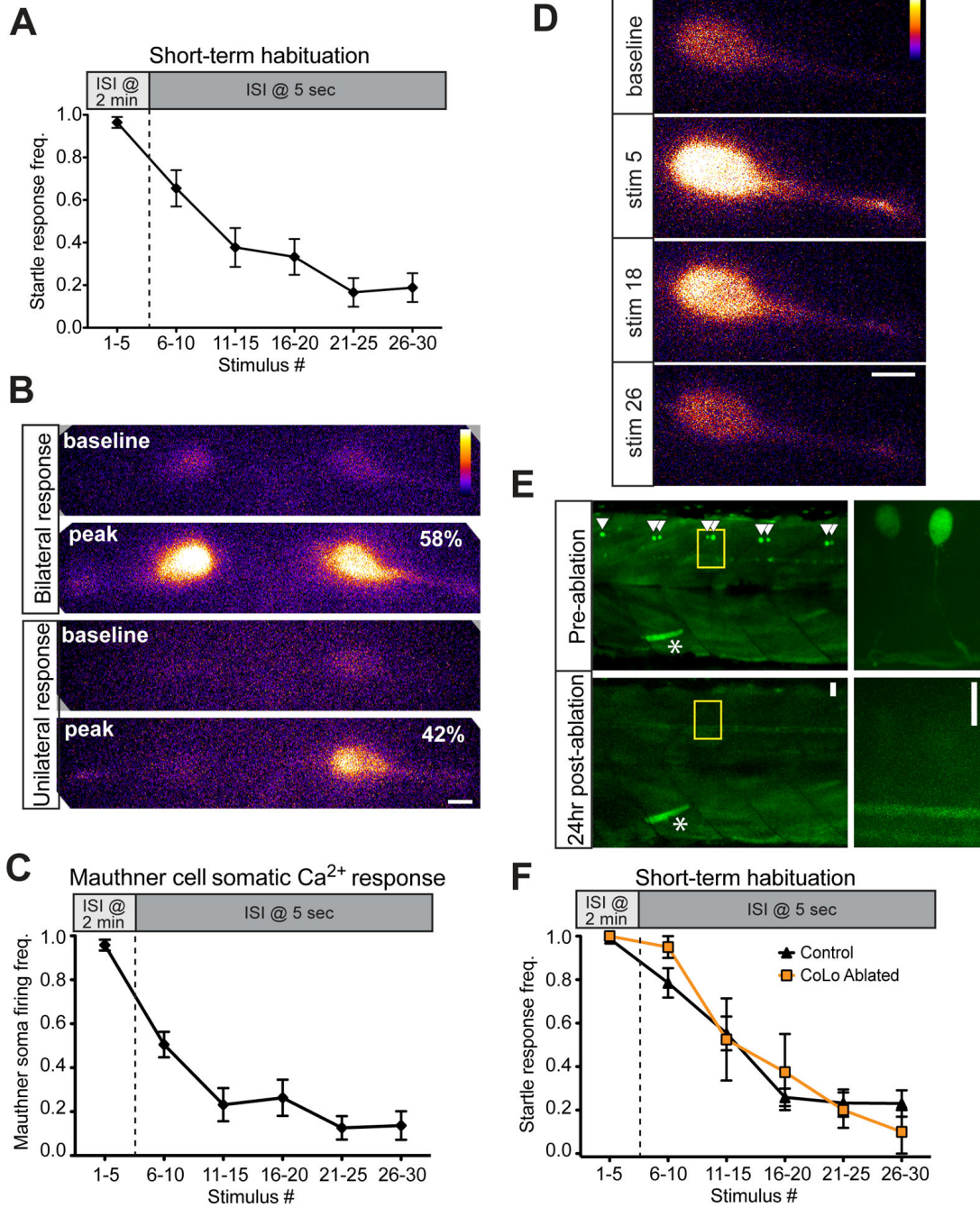
****$p<0.0001$, one-way ANOVA with Dunnett's Multiple Comparison Test). (D) Scatterplot of peak lateral dendrite $\Delta F/F_0$ with startle events in red and no startle events in white. Grey bar indicates the lateral dendrite activation threshold for startle behavior.

Figure 3. Inhibition downstream of M-cell does not cause startle habituation

(A) A 30-stimulus assay (5 pulses @ 2 min ISI, 25 pulses @ 5 s ISI) induced robust startle habituation in head-restrained larvae. (B) 40× magnification images of bilateral M-cell GCaMP6s labeling demonstrate unilateral (bottom, 42%) and bilateral (top, 58%) M-cell firing (n=50 responses from 5 fish; scale bar 10 μm). (C) The frequency of M-cell somatic Ca^{2+} responses during short-term habituation is strongly reduced during habituation. (D) Representative images show baseline and peak fluorescence for non-habituating (stim 5) and habituating stimuli (stim 18 and 26; scale bar 10 μm). (E) Representative images at 10×

(left) and 63× (right) show pre-ablation labeling of CoLo interneurons and their absence 24 hrs postablation. Asterisk highlights a GFP-labeled muscle cell to indicate the same segments are imaged pre- and post-ablation (scale bar 10 μm). (F) Both control and CoLo-ablated larvae rapidly habituate to repeated acoustic stimulation.
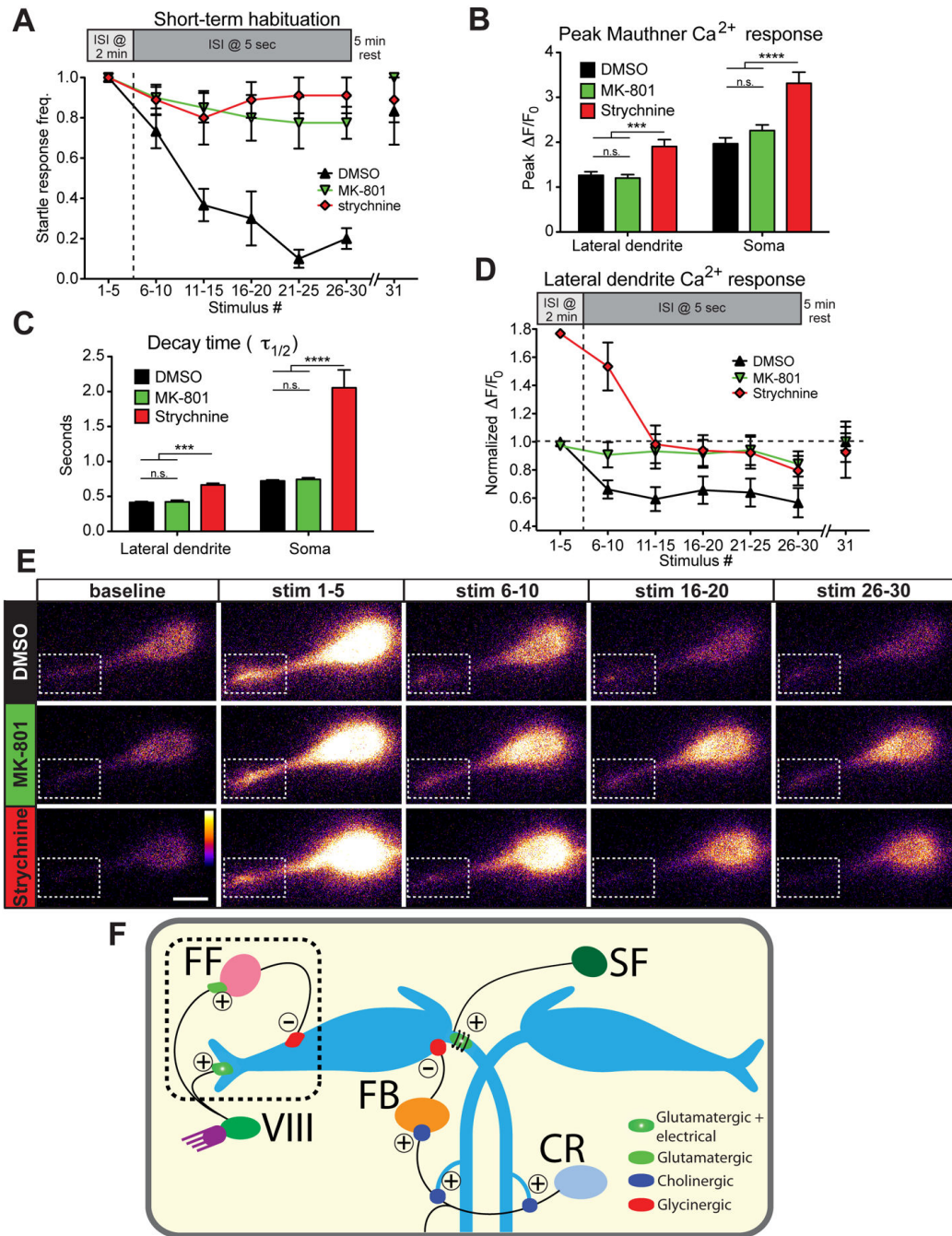
Figure 4. PSP depression drives short-term startle habituation

(A) 500 μM MK-801 (n=8) and 100 μM strychnine (n=9) strongly reduce short-term habituation of the startle response compared to DMSO-treated controls (n=8). A 5 min rest period allows complete recovery to the 31st stimulus. (B) Peak F/F_0 levels in M-cell lateral dendrite and soma are unaffected by MK-801 but are increased by strychnine (***$p<0.001$, ****$p<0.0001$, t-test). (C) Ca^{2+} signal decay kinetics are unaltered by MK-801 but are increased by strychnine (***$p<0.001$, ****$p<0.0001$, t-test). (D) Normalized M-cell lateral dendrite Ca^{2+} responses are decreased ~35% in DMSO-treated fish during habituation while

MK-801 treatment prevented this decrease (****$p<0.0001$, 2-way ANOVA). Responses in strychnine-treated larvae decreased from a higher baseline but remained elevated compared DMSO-treated larvae (****$p<0.0001$, 2-way ANOVA). (E) Representative images for each block of 5 stimuli show PSP depression in DMSO compared to MK-801-and strychnine-treated fish. (Dashed box highlights lateral dendrite; scale bar 10 μm). (F) Diagram of the M-cell circuit including known regulatory inputs. Startle habituation arises from an NMDA- and glycine-receptor dependent mechanism that likely results in enhanced transmission from feedforward (FF) inhibitory neurons to the M-cell and may involve depression of acoustic nerve (VIII) inputs to the M-cell. Inputs from downstream spiral fiber (SF), cranial relay (CR), and feedback inhibitory (FB) neurons are most likely not involved in startle habituation. Excitatory (+) and inhibitory (−) connections are labeled.